



Use of Satellite-based Leaf Area Index Data for Monitoring Green Gram Crop Growth in Ikombe-Katangi Area, Machakos County, Kenya

Manzi, K. H. ^{a*}, Shadrack Ngene ^b
and Joseph, P. Gweyi-Onyango ^a

^a Department of Agriculture Science and Technology, Faculty of Agriculture, Kenyatta University, Kenya.

^b Kenya Wildlife Service, Spatial Ecology and Biodiversity Monitoring, Kenya.

Authors' contributions

This work was carried out in collaboration among all authors. All authors read and approved the final manuscript.

Article Information

DOI: 10.9734/AJAAR/2023/v23i3468

Open Peer Review History:

This journal follows the Advanced Open Peer Review policy. Identity of the Reviewers, Editor(s) and additional Reviewers, peer review comments, different versions of the manuscript, comments of the editors, etc are available here: <https://www.sdiarticle5.com/review-history/108087>

Original Research Article

Received: 13/08/2023

Accepted: 17/10/2023

Published: 20/10/2023

ABSTRACT

Monitoring the conditions under which crops grow and estimating their yield is essential to the process of economic development in any nation. The traditional approaches to crop monitoring are labor- and resource-intensive, as well as limited in their ability to cover expansive geographic regions. Since remote sensing data is integrated with ground measurements, it has been used as a potentially useful tool to extract biophysical variables such as leaf area index (LAI), biomass, and phenology. Leaf Area Index (LAI) is a key variable that bridges remote sensing observations to the quantification of agroecosystem processes such as yield. The potential of satellite-based LAI for monitoring crop growth was investigated and compared to field measurements. This was the

*Corresponding author: Email: manzikye@gmail.com;

objective of his study. High resolution leaf area index was retrieved from Landsat 8 OLI imageries, and ground leaf area index measurements were taken in Ikombe-Katangi Machakos in Machakos county. An equation based on regression was developed to estimate the leaf area index using the normalized difference vegetation index that was derived from Landsat-8 OLI (NDVI). According to the findings, the derived LAI exhibited strong linear relationships with the leaf area index that was measured on the ground for green gram crops, with RMSE values being 0.09846, and R2 values of 0.9249. The overall findings shed light on the viability of using multispectral data, in estimating leaf area index in a very fragmented agricultural landscape, such as that found in the Ikombe and Katangi areas of Machakos, Kenya. Therefore, accurate crop monitoring on a large scale can be accomplished through remote sensing data in conjunction with LAI measurements taken from the ground. The implementation of the leaf area index is subject to the environmental condition which requires to be investigated as the use of remote sensing data is advocated for. The advancement in the use of satellite data for extraction LAI data is key towards transforming crop production within Kenya and Africa at large. Scarce resources for crop growth monitoring can now be augmented with open-source satellite datasets such as Landsat 8 in LAI estimation.

Keywords: Leaf area index; satellite data; normalized vegetation index; enhanced vegetation index; landsat 8; remote sensing.

1. INTRODUCTION

The leaf area index, or LAI, is a measurement that can be used to quantify the amount of live green leaf material that is present in the canopy of a given area. It is utilized in the estimation of photosynthesis, evapotranspiration, crop yield, and other physiological processes in the field of agroecosystem research [1].

The Leaf Area Index (LAI) is a non-dimensional measurement that is based on the ratio of the leaf area on one side (measured in m²) to the ground surface area (measured in m²) [2]. The leaf area index (LAI) has long been recognized as a good indicator for a variety of agronomic, ecological, and hydrological applications. Modeling atmospheric circulation [3], photosynthesis and biomass accumulation [4], and evapotranspiration are some examples of these applications [4]. Other applications include determining the state of the surrounding vegetation (Reyes) [5].

Remote sensing has proven to be a promising alternative tool for estimating crop LAI quickly and without causing damage to the canopy [6,7]. There are two approaches to obtaining crop biophysical variables from remote sensing: empirical and physical modelling. The LAI-VI approach is the simplest method of estimating LAI from remote sensing. It involves establishing an empirical relationship between remotely sensed vegetation indices (VIs) and measured LAI [8,9]. Historically, LAI was measured using in situ accurate LAI measurements; however, with the advent of remote sensing technologies, both

in situ measurements and remotely sensed data are used in tandem to establish the best LAI-VI relationships that can be used to estimate LAI, particularly over large areas [10].

Agriculture contributes significantly to Kenya's economy and is critical to ensuring food security [11]. Due to limited resources, gathering data for crop monitoring in semi-arid areas of Katangi and Machakos has been difficult. Continuous data measurements for proper crop growth monitoring have been a problem in this case. This has limited the local government's ability to monitor crop production and food security in the area.

The research study objective was to look at the potential for the satellite derived LAI data in monitoring crop growth in green gram in Katangi, Machakos area. The need to use satellite data for crop monitoring amidst scarce resource in semi-arid areas of Kenya is necessary. Perennial food crisis in this region has made it difficult for the local government to plan due to accurate data on crop production. The null hypothesis was that a negative correlation existed between satellite derived and field measurement LAI data. Technologies such as remote sensing data enable informed decisions on food security issues and timely availability of information on agriculture.

1.1 Study Area

According to Fig. 1, the wards of Katangi and Ikombe in Machakos County, Kenya was the focus of this research (1°16'24.55"S; 37°40'13.30"E). The climate of the study region

can be summarised as being very dry and hot on average. The Arid and Semi-Arid Lands (ASALs) are a region that can be found in the eastern part of the Sudano-Sahelian belt. This region is made up of a variety of land types, such as coastal plains, upland plateaux, and isolated hill ranges, and is primarily located at an elevation of less than 1600 metres [12]. The arid regions are characterized by high average temperatures with a large range in temperature throughout the day. Rainfall in these regions is scant, sporadic, and of two modes, and it varies greatly in both location and over the course of time [13]. The majority of rain comes in the form of intense but brief storms, which are responsible for significant amounts of runoff and soil erosion. The arid areas typically receive between 150 and 450 millimetres of precipitation throughout the course of a year on average. The soils are extremely variable, but in general they are shallow, of light to medium texture, with low fertility, and they are susceptible to compaction, capping, and erosion [14]. The cultivation of crops is only possible in a select few locations due to the presence of volcanic soils and alluvial deposits. Heavy clays can also be found but cultivating them is challenging due to the poor workability of the clays as well as the salinity and sodicity issues that they present. Both the availability of water and its accessibility are highly variable, which is a significant factor that inhibits production [14] and at the same time encourages the growing

low water demanding crops such as green grams.

The study area is located within agroecological zones (AEZ) IV and V-VI, and it receives an annual rainfall totaling anywhere from 500 to 850 millimetres. They are then divided even further into four categories, based on their potential for agricultural use [14]. These include a) semi-arid areas with mixed rain-fed and irrigation agriculture as well as high economic and political disparities; b) semi-arid areas with encroaching agro-pastoral use by marginalized smallholders; c) semi-arid areas with predominantly pastoralist use in the economic and political periphery; and d) semi-arid areas that include protected areas and their surrounding areas. Semi-arid conditions can be found in the counties of Kajiado, Narok, Mbeere, Mwingi, Kitui, Machakos, and Makueni [12].

Mixed crop and livestock production is the primary form of agriculture practiced in these regions. Crops are grown to satisfy the subsistence needs of the household, and any surplus is sold for monetary gain to supplement the income of the household [11]. The lack of rainfall and the high number of pests both present significant dangers. Farmers who keep livestock, engage in mixed cropping, and plant drought-resistant crops such as cow and pigeon peas can reduce the impact of these risks on their businesses [15].

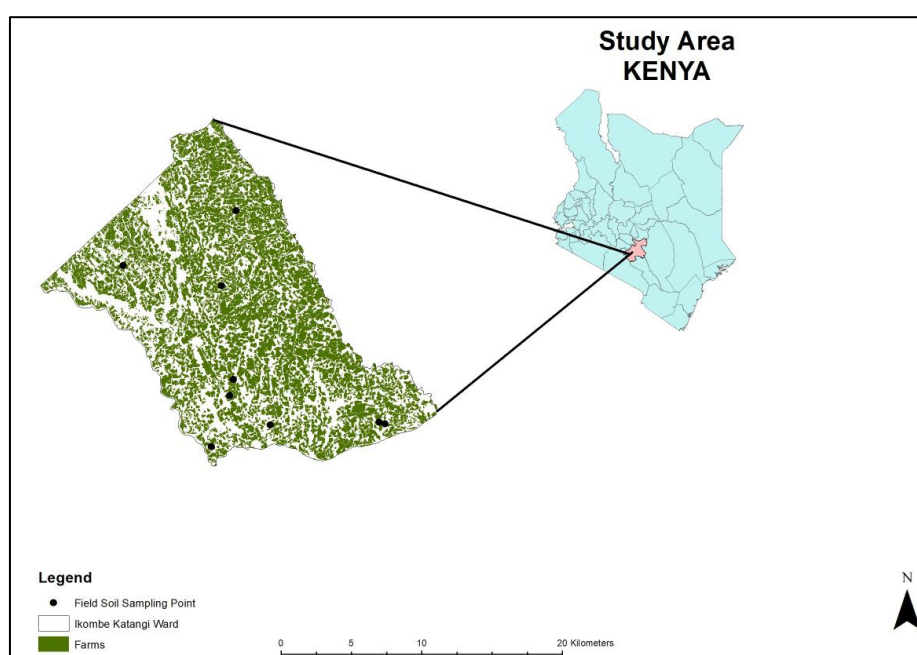


Fig. 1. Map showing study area in Kenya

2. METHODS

The analysis of the Leaf Area Index was undertaken at the vegetative stage of the crop which was guided by the growth stage classification of the study area which is shown in Table 1. The rains for the October to December season delayed and started off in November.

2.1 Image Acquisition and Preprocessing

The research used Landsat 8 data for the long rain season for 2020, within the study area. Multi-temporal Landsat data have been found to be very useful in crop monitoring. NASA Landsat-8 satellites provide images every 16 days with a spatial resolution of 30m [16]. The acquired data considered images within the same temporal resolution. Additionally, the landscape vector data for this the study area was acquired from Kenya's administrative ward data to aid in the extraction of the area of interest in the satellite imagery.

The collection of 2 level one satellite images of the Landsat-8 OLI products that were used within the scope of this study were obtained from the website of the American Geological Service (USGS) with orthorectification and radiometric correction [17]. The images were in the Universal Transverse Mercator (UTM) coordinate system, and geometric corrections were made to position

them on 37 South and the WGS84 datum.). The metadata of the images used is presented in (Table 2).

2.2 Leaf Area Index Calculation Using Satellite Data

The vegetation index (VI) approach associated with spectral vegetation indices was used to estimate the LAI. This approach establishes a statistical relationship between remotely sensed VIs and observed LAI values, [18]. At the beginning, normalized difference vegetation index (NDVI) and soil-related vegetation index (SR) were commonly used. Over the years, other vegetation indices have been developed; they include; Soil Adjusted Vegetation Index(SAVI), [18,6], Atmospherically Resistant Vegetation Index (ARVI) [19], Enhanced Vegetation.

To estimate LAI, the vegetation index approach has been adopted as its easy and simple to calculate. The main challenge is the lack of In situ LAI measurement that can be used to make an LAI-VI relationship that is in accordance with the study area. Therefore, a method to calculate the LAI has been adopted from an existing LAI-VI index, . The equation for leaf area determination is as follows; ,

$$LAI=(2.77\sqrt{EVI2(1.66)})^{(3/2)} \tag{1}$$

Table 1. Phenological growth stage of plant from October to February

Phenological growth stage	Month				
	October	November	December	January	February
Germination, sprouting, bud development	Mid to End of October	Early November			
Leaf development/ shoot development.	End of October	Early to Mid-November			
Development of vegetative plant parts, bolting		Late November	Early to late December	Early to mid-January	
Inflorescence emergence, Flowering /Pod filling			Late December	Early to mid January	
Harvesting				Late January	Mid-February to late February

Table 2. Landsat 8 OLI scene satellite imagery imagery metadata

Landsat 8 product	Type of product	Path	Row	Date of acquisition	Cloud cover
LC08_L1TP	Collection 2 level 1	168	61	20/12/2020	1.30

Table 3. Crop coefficient for various crops vegetation indices [20]

Crop Type	VI	SLR Model	Coefficient (Confidence Interval)		Prediction Model	RMSE (m ² /m ²)	MAE (m ² /m ²)	Quantiles of Absolute Residuals (m ² /m ²)				
			a	b				5%	25%	50%	75%	95%
Overall	EVI	$\sqrt{y} = ax + b$	2.07 (1.97, 2.17)	0.47	$y = (ax + b)^2$	1.13	0.89	0.06	0.33	0.70	1.38	2.24
	EVI2	$\sqrt{y} = a\sqrt{x} + b$	2.92 (2.78, 3.06)	-0.43	$y = (a\sqrt{x} + b)^2$	1.11	0.87	0.06	0.32	0.70	1.33	2.17
Row crop	EVI	$\sqrt{y} = ax + b$	2.16 (2.1, 2.32)	0.41	$y = (ax + b)^2$	1.14	0.89	0.06	0.31	0.67	1.32	2.29
	EVI2	$\sqrt{y} = a\sqrt{x} + b$	3.16 (3.01, 3.31)	-0.58	$y = (a\sqrt{x} + b)^2$	1.12	0.86	0.06	0.30	0.67	1.28	2.22
Maize	EVI	$\sqrt{y} = ax + b$	2.42 (2.21, 2.65)	0.34	$y = (ax + b)^2$	1.01	0.81	0.07	0.33	0.72	1.15	1.98
	EVI2	$y^{\frac{1}{2}} = a\sqrt{x} + b$	5.3 (4.89, 5.68)	-1.66	$y = (a\sqrt{x} + b)^{\frac{1}{2}}$	0.92	0.74	0.06	0.29	0.65	1.02	1.81
Soybean	EVI	$\sqrt{y} = ax + b$	2.53 (2.28, 2.76)	0.08	$y = (ax + b)^2$	0.69	0.49	0.02	0.14	0.32	0.68	1.45
	EVI2	$\sqrt{y} = a\sqrt{x} + b$	2.77 (2.47, 3.03)	0.06	$y = (ax + b)^2$	0.70	0.51	0.04	0.15	0.34	0.78	1.42
Wheat	EVI	$y^{\frac{1}{2}} = ax + b$	4.24 (3.71, 4.78)	0.22	$y = (ax + b)^{\frac{1}{2}}$	1.13	0.94	0.07	0.41	0.82	1.34	2.03
	EVI2	$y^{\frac{1}{2}} = ax^{\frac{1}{2}} + b$	5.47 (4.81, 6.16)	-1.03	$y = (ax^{\frac{1}{2}} + b)^{\frac{1}{2}}$	1.13	0.94	0.12	0.41	0.87	1.37	2.12
Rice	EVI	$y^{\frac{1}{2}} = ax + b$	4.27 (3.25, 5.23)	-0.05	$y = (ax + b)^{\frac{1}{2}}$	1.03	0.79	0.07	0.35	0.67	1.02	2.38
	EVI2	$y^{\frac{1}{2}} = ax + b$	5.32 (4.08, 6.51)	-0.18	$y = (ax + b)^{\frac{1}{2}}$	1.02	0.78	0.06	0.34	0.70	1.06	2.35
Cotton	EVI	$\sqrt{y} = a\frac{1}{\sqrt{x}} + b$	-1.25 (-1.39, -1.11)	2.97	$y = (a\frac{1}{\sqrt{x}} + b)^2$	0.91	0.73	0.05	0.25	0.55	1.12	1.62
	EVI2	$\sqrt{y} = a\frac{1}{\sqrt{x}} + b$	-1.21 (-1.33, -1.07)	2.95	$y = (a\frac{1}{\sqrt{x}} + b)^2$	0.93	0.76	0.04	0.33	0.64	1.16	1.61
Pasture	EVI	$y^{\frac{1}{2}} = ax^2 + b$	2.84 (2.49, 3.20)	0.88	$y = (ax^2 + b)^{\frac{1}{2}}$	0.98	0.81	0.10	0.45	0.72	1.07	2.00
	EVI2	$y^{\frac{1}{2}} = ax^{\frac{1}{2}} + b$	2.99 (2.6, 3.37)	0.72	$y = (ax^{\frac{1}{2}} + b)^{\frac{1}{2}}$	0.99	0.82	0.06	0.42	0.70	1.12	1.91

According to Kang et al., 2016, it was possible to establish that saturation is less common in relationships using EVI and EVI2 compared to NDVI, and in some cases EVI and EVI2 are linearly related to LAI, indicating an ability to resolve LAI differences over a wider range of canopy conditions. EVI2 was found to perform better than EVI in prediction power across all crops, proving that it can be used as a strong estimator of LAI when data from the blue band are not available. In this case, the global LAI-VI relationships that were built by [20], in Table 3 shows the LAI-VI relationships for specific crops as obtained from the study. It is from these relationships that equation 1 was performed that estimates the LAI of green gram crop using EVI2 vegetation index. For green gram, the coefficients for soy bean were used due to the similarity in leaf characteristics.

Landsat 8 OLI band data was acquires from the Glovis website and converted to TOA planetary reflectance using reflectance rescaling coefficients provided in the product meta-data file (MTL file). The following equation was used to the convert the DN values to TOA reflectance for Landsat 8OLI data as follows:

$$pA' = Mp * Qcal + Ap$$

Where:

pA' = TOA planetary reflectance, without correction for solar angle. Note that pA' does not contain a correction for the sun angle.

Mp = Band-specific multiplicative rescaling factor from the metadata (REFLECTANCE_MULT_BAND_x, where x is the band number).

Ap = Band-specific additive rescaling factor from the metadata (REFLECTANCE_ADD_BAND_x, where x is the band number)

Qcal = Quantized and ca liberated standard product pixel values (DN) TOA reflectance with a correction for the sun angle is then:

$$pA = pA' / \cos(\theta_{sz}) = pA' / \sin(\theta_{se})$$

Where

pA = TOA planetary reflectance theta_se= Local sun elevation angle. The scene center sun elevation angle in degrees is provided in the meta-data (SUN_ELEVATION).

theta_sz = Local so lar zenith angle; theta_sz=90- theta_se

The atmospherically corrected image was cropped to the extents of the study area.

The EVI formula was applied to the georeferenced image to obtain EVI values of the image using any GIS platform ARCGIS10.8.

$$EVI = 2.5 * ((Band 5 - Band 4) / (Band 5 + 6 * Band 4 - 7.5 * Band 2 + 1)) \quad (2)$$

In ARCGIS 10.8 the EVI value was calculated using the model builder tool through the calculate value tool, which allows the use of the Python math module to perform more complex mathematical operations. Once the EVI values were obtained. The EVI formulas used were; $EVI = G * \rho_{NIR} - \rho_{RED} \rho_{NIR} + (C1 * \rho_{RED} - C2 * \rho_{BLUE}) + L$

and can be rewritten as;

$$EVI = G * \rho_{NIR} / \rho_{RED} - 1 * \rho_{NIR} / \rho_{RED} + (C1 - C2 * \rho_{RED} / \rho_{RED}) + L / \rho_{RED}$$

Where:

L is a soil adjustment factor,

C1 and C2 are coefficients used to correct aerosol scattering in the red band using the blue band. The ρ_{blue} , ρ_{red} , and ρ_{nir} represent reflectance in the blue (0.45-0.52 μ m), red (0.6-0.7 μ m)

Near-Infrared (NIR) wavelengths (0.7-1.1 μ m)

G is a gain factor.

In Landsat 8 the equation would be formulated as follows.

$$EVI = 2.5 * ((BAND5 - BAND4) / (BAND5 + 6 * BAND4 - 7.5 * BAND2 + 1))$$

where NIR corresponds to the near-infrared band (LANDSAT band 4), RED corresponds to

The red band (LANDSAT band 3), BLUE corresponds to the blue band (LANDSAT band 1).

2.3 Field Measurement of Leaf Area Index

Under field measurement, an area of 3 by 3 m was identified for the harvesting of leaves for the measurements of LAI. Direct methods for determining leaf area were used. This involved harvesting all the leaves and calculating the leaf area which was later used to determine the LAI [21]. Measuring leaf area index. LAI was measured for the vegetative season where the satellite data was also available from areas in representative plots. The formula used in calculation is documented in equation 1.

$$LAI = \frac{(\text{Dry Weight Sampling area})}{(\text{Sampling area})} * \frac{(\text{Leaf Area})}{(\text{Leaf Dry Weight})} \quad (3)$$

3. RESULTS

Leaf Area Index parameters was extracted from remote sensing-based data for green gram under farm field conditions. The leaf area index was calculated and validated using field results from the two study areas. The LAI ranged from 1.068 to 1.77 for green gram and while field data results ranged from 1.066 to 1.833, see Fig. 2. The observed LAI from field data and the estimated LAI from satellite data is shown in Table 4. The correlation analysis was carried out between the field and satellite data and RMSE error of 0.09846 and R2 of 0.9249. The patterns of the changing Leaf area index for green gram can be observed in Fig. 2 while the analysis of the correlation between the results is well displayed in Fig. 3.

Table 4. Field and remote sensing extracted leaf area index data

CROP	Observed LAI	Estimated LAI
Green Gram	1.068	1.2333
Green Gram	1.13315	1.100
Green Gram	1.7425	1.8667
Green Gram	1.07165	1.0667
Green Gram	1.25095	1.3333
Green Gram	1.67	1.8333
Green Gram	1.77275	1.7667
Green Gram	1.7472	1.7333
rmse	0.09846	

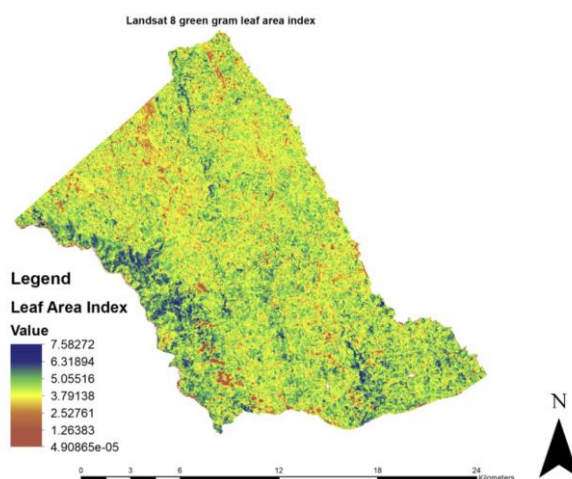


Fig. 2. Extracted leaf area index data for green gram crop in Ikombe-Katangi study area

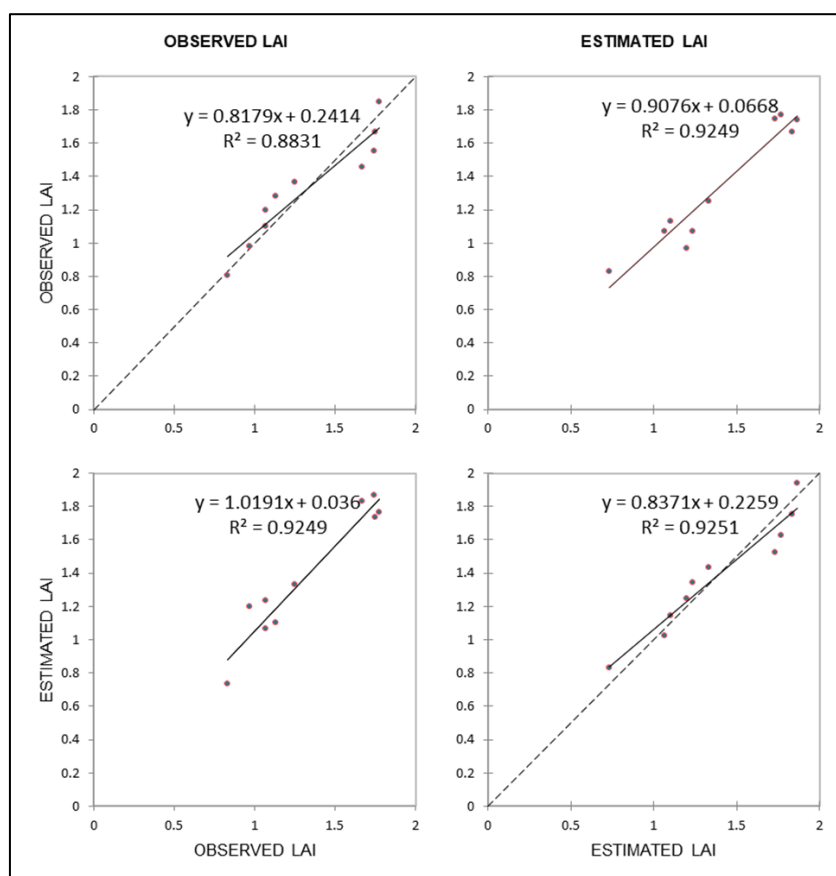


Fig. 3. R2 results for remote sensing-based leaf area index correlations with green gram field data

4. DISCUSSION

Leaf Area Index (LAI), which is the total green leaf area (double-sided) per unit horizontal ground surface area of vegetation canopy [22,23] is an essential biophysical variable. It is used in

soil-vegetation-atmosphere modeling [24-26,18]. In agroecosystems, the total leaf area of the crop canopy, is one of the key constraints on carbon assimilation and transpiration rates, which drive the accumulation of crop primary productivity [27] Therefore, LAI is required to estimate

photosynthesis, evapotranspiration, crop yield, and many other physiological processes [28]. EVI2 has frequently been used for crop growth and yield-related research as a remote sensing parameter [29-32]. EVI-based crop growth metrics are much closer to capture crop status and growth characteristics, and growth metrics can be much more correlated to crop yield than an NDVI, [33]. Similarly, this study used EVI indices to ensure that the crop yield estimation would be accurate.

LAI is one of the important parameters that reflects crop growth stages of vegetation and is widely used in quantitative analysis of crop models [34,35]. Parker [36], reiterates on the importance of leaf area index (LAI) by discussing remote sensing models used in its estimation. Several studies have extracted biophysical parameters from satellite imagery [37,38] and assimilated them in simulation models. [39], successfully assimilated Landsat-derived LAI time series into crop model simulations using ensemble Kalman filter for individual fields or pixels. The covariance correlation matrix between the extracted and observed data for the LAI was R^2 0.92549 for green gram as shown in Fig. 3. The results used in the correlation matrix is shown in Table 4. The results showed a high correlation between satellite data estimated LAI and the field measured LAI. The estimate LAI values in Table 4 were either slightly higher or sometimes slightly lower from field measurements but differences in the data was not huge. This is an indication that satellite derived LAI can give accurate results for crop monitoring. Klinger et al. [40] in the study on LAI estimation on grasslands using different methods, showed a high correlation in the indirect optical methods. Confirming the validity of using satellite data in estimating the Leaf Area Index. Monitoring of the vegetation structure and function can be accomplished through spectral and remote sensing data, The implication of these findings is that the possibility of enhancing crop monitoring in much easier and cheaper methods is possible. The possibility of monitoring crop production and further addressing food security in the advent of climate change is possible through remote data [41].

5. CONCLUSIONS

LAI-VI relationships vary depending on crop, and the EVI or EVI2 derived from surface reflectance are the most accurate measures to use [10]. The most important contribution of this work is

confirmation that satellite LAI can provide accurate data for crop growth monitoring in regions where crop monitoring resources are limited. The free availability of datasets like Landsat 8 provides desperately needed resources for crop monitoring in semi-arid regions vulnerable to climate change. The ease with which VI can be generated using remotely sensed images and the application of simple statistical relationships adds to the research's practical value. This is especially true when essential variables required for process-based methods are scarce and difficult to measure in small-holder farm field conditions. Furthermore, the findings of this study would be useful in addressing significant concerns about monitoring food security in semi-arid regions.

The lack of multiple images to compare the LAI index across different stages of growth limited the research. A comparison of LAI from Landsat 8 and Sentinel data would advance this study and provide guidance on different spatial accuracy in estimating LAI for semi-arid regions.

COMPETING INTERESTS

Authors have declared that no competing interests exist.

REFERENCES

1. Demarty J, Chevallier F, Friend AD, Viovy N, Piao S, Ciais P. Assimilation of global MODIS leaf area index retrievals within a terrestrial biosphere model. *Geophysical Research Letters*. 2007;34(15). DOI:10.1029/2007GL030014.
2. DOI:10.1029/2007GL030014.
3. Asner GP, Scurlock JMO, Hicke JA. Global synthesis of leaf area index observations: Implications for ecological and remote sensing studies. *Glob. Ecol. Biogeogr.* 2003;12:191–205.
4. Reyes-González A, Kjaersgaard J, Trooien T, Sánchez DGR, Sánchez-Duarte JI, Preciado-Rangel P, Fortis-Hernandez M. Comparison of Leaf Area Index, Surface Temperature, and Actual Evapotranspiration Estimated using the METRIC Model and In Situ Measurements. *Sensors*. 2019;19:1857.
5. Fassnacht KS, Gower ST, MacKenzie MD, Nordheim EV, Lillesand TM. Estimating the leaf area index of North Central Wisconsin forests using the landsat thematic mapper. *Remote. Sens. Environ.* 1997;61: 229–245.

6. Jung M, Reichstein M, Ciais P, Seneviratne SI, Sheffield J, Goulden ML, Bonan G, Cescatti A, Chen J, De Jeu R, et al. Recent decline in the global land evapotranspiration trend due to limited moisture supply. *Nature* 2010;467:951–954.
7. Qi J, Kerr YH, Moran MS, Weltz M, Huete AR, Sorooshian S, Bryant R. Leaf area index estimates using remotely sensed data and BRDF models in a semiarid region. *Remote Sensing of Environment*. 2000;73(1):18–30.
8. Available:[https://doi.org/10.1016/S0034-4257\(99\)00113-3](https://doi.org/10.1016/S0034-4257(99)00113-3)
9. Mourad R, Jaafar H, Anderson M, Gao F. Assessment of leaf area index models using harmonized landsat and sentinel-2 surface reflectance data over a semi-arid irrigated landscape. *Remote Sensing* 2020;12:3121,12(19), 3121.
10. Available:<https://doi.org/10.3390/RS12193121>
11. Baret F, Guyot G. Potentials and limits of vegetation indices for LAI and APAR assessment. *Remote. Sens. Environ*. 1991;35:161–173.
12. Broge N, Leblanc E. Comparing prediction power and stability of broadband and hyperspectral vegetation indices for estimation of green leaf area index and canopy chlorophyll density. *Remote. Sens. Environ*. 2001;76:156–172.
13. Kinane SM, Montes CR, Albaugh TJ, Mishra DR. A model to estimate leaf area index in loblolly pine plantations using landsat 5 and 7 images. *Remote Sensing*. 2021;13(6).
14. Available:<https://doi.org/10.3390/RS13061140>
15. Gichangi, E. M., Gatheru, M., Njiru, E. N., Mungube, E. O., Wambua, J. M., & Wamuongo, J. W. (2015). Assessment of climate variability and change in semi-arid eastern Kenya. *Climatic Change*, 130(2), 287–297. <https://doi.org/10.1007/s10584-015-1341-2>
16. Republic of Kenya. *Machakos District Development Plan 2002-2008: Effective Management for Sustainable Economic Growth and Poverty Reduction*. Nairobi, Kenya: Government Printer; 2002
17. Shisanya CA, Recha C, Anyamba A. Rainfall Variability and Its Impact on Normalized Difference Vegetation Index in ASALs of Kenya. *International Journal of Geosciences*. 2011;2:36-47.
18. Jaetzold R, Schmidt H. *Farm Management Handbook of Kenya: National Conditions and Farm Management Information, Vol. II: Part A. Western Kenya*. Nairobi: Ministry of Agriculture; 1983.
19. Republic of Kenya. *Mainstreaming Sustainable Land Management in Agro-Pastoral Production Systems of Kenya*. UNDP Project Document-UNDP PIMS NO.3245, GEF ID 3370; 2010.
20. Immitzer, Vuolo, Atzberger. First experience with Sentinel-2 data for crop and tree species classifications in central Europe. *Remote Sensing*. 2016;8(3) 166.(3):166.
21. Available:<https://doi.org/10.3390/>
22. Nasa U.S. Geological Survey. *Landsat Data Continuity Mission*. USA: USGS; 2013.
23. Anav A, Murray-Tortarolo G, Friedlingstein P, Sitch S, Piao S, Zhu Z. Evaluation of land surface models in reproducing satellite derived leaf area index over the high-latitude northern hemisphere. Part II: Earth System Models. *Remote Sens*. 2013;5:3637–3661
24. Kaufman YJ, Tanré D. Atmospherically Resistant Vegetation Index (ARVI) for EOS-MODIS. *IEEE Transactions on Geoscience and Remote Sensing*. 1992;30(2):261–270.=
25. Available:<https://doi.org/10.1109/36.134076>
26. Kang Y, Özdoğan M, Zipper SC, Román MO, Walker J, Hong SY, Marshall M, Magliulo V, Moreno J, Alonso L, Miyata A, Kimball B, Loheide SP. How Universal Is the Relationship between Remotely Sensed Vegetation Indices and Crop Leaf Area Index? A Global Assessment. *Remote Sensing* 2016;8:5978(7);597.
27. Available:<https://doi.org/10.3390/RS8070597>
28. Manivel L, Weaver RJ. Effect of growth regulators and heat on germination of Tokay grape seeds. *Vitis*. 1974;12(4):286-90.
29. Watson DJ. Comparative physiological studies on the growth of field crops: I. variation in net assimilation rate and leaf area between species and varieties, and within and between years. *Ann. Bot*. 1947;11:41–76.
30. Fernandes R, Plummer S, Nightingale J, Baret F, Camacho F, Fang H, Garrigues S, Gobron N, Lang M, Lacaze R, et al. Global leaf area index product validation good

- practices. Version 2.0. Best Practice for Satellite-Derived Land Product Validation; Schaepman-Strub, G., Román, M., Nickeson, J., Eds.; Land Product Validation Subgroup (WGCV/CEOS). 2014;76.
31. Available: <http://lpvs.gsfc.nasa.gov/documents.html>
 32. Laurent VCE, Schaepman ME, Verhoef W, Weyermann J, Chávez RO. Bayesian object-based estimation of LAI and chlorophyll from a simulated Sentinel-2 top-of-atmosphere radiance image. *Remote Sensing of Environment*. 2014;140 (0):318–329.
 33. Available:<https://doi.org/10.1016/j.rse.2013.09.005>
 34. Launay M, Gueri. Assimilating remote sensing data into a crop model to improve predictive performance for spatial applications. *Agric. Ecosyst. Environ*. 2005;111:321–339. [CrossRef]
 35. Food and Agriculture Organization of the United Nations (FAO). *Terrestrial Essential Climate Variables for Climate Change Assessment, Mitigation and Adaptation*; FAO: Rome, Italy; 2008
 36. Gitelson AA. Wide dynamic range vegetation index for remote quantification of biophysical characteristics of vegetation. *Journal of Plant Physiology*. 2004;161(2):165–173.
 37. Available:<https://doi.org/10.1078/0176-1617-01176>
 38. Cao X, Zhou Z, Chen X, Shao W, Wang Z. Improving leaf area index simulation of IBIS model and its effect on water carbon and energy—A case study in Changbai Mountain broadleaved forest of China. *Ecol. Model*. 2015;303:97–104
 39. Kogan F, Salazar L, Roytman L. Forecasting crop production using satellitebased vegetation health indices in Kansas, USA. *Int. J. Remote Sens*. 2012;33:2798–2814.
 40. Available:<https://doi.org/10.1080/01431161.2011.621464>
 41. Zhang HK, Chen JM, Huang B, Song HH, Li YR. Reconstructing seasonal variation of Landsat vegetation index related to leaf area index by fusing with MODIS data. *IEEE Journal of Selected Topics in Applied Earth Observations and Remote Sensing*. 2014;7(3):950–960.
 42. Available:<https://doi.org/10.1109/jstars.2013.2284528>
 43. Huang X, Liu J, Zhu W, Atzberger C, Liu Q. The optimal threshold and vegetation index time series for retrieving crop phenology based on a modified dynamic threshold method. *Remote. Sens*. 2019;11(23):2725.
 44. Available:<https://doi.org/10.3390/rs11232725>.
 45. Liu Q, Liang S, Xiao Z, Fang H. Retrieval of leaf area index using temporal, spectral, and angular information from multiple satellite data. *Remote Sensing of Environment*. 2014;145(0): 25–37.
 46. Available:<https://doi.org/10.1016/j.rse.2014.01.021>
 47. Huang X, Liu J, Zhu W, Atzberger C. Liu Q. The optimal threshold and vegetation index time series for retrieving crop phenology based on a modified dynamic threshold method. *Remote. Sens*. 2019;11(23):2725.
 48. Available:<https://doi.org/10.3390/rs11232725>.
 49. Parker Geoffrey G. Tamm review: Leaf area index (LAI) Is both a determinant and a consequence of important processes in vegetation canopies. *Forest Ecology and Management* 2020;477.
 50. Available:<https://doi.org/10.1016/j.foreco.2020.118496>.
 51. Yan Guangjian, Ronghai Hu, Jinghui Luo, Marie Weiss, Hailan Jiang, Xihan Mu, Donghui Xie, and Wuming Zhang. Review of indirect optical measurements of leaf area index: Recent advances, challenges, and perspectives. *Agricultural and Forest Meteorology*. 2019;265 (March 2018):390–411.
 52. Available:<https://doi.org/10.1016/j.agrforme.2018.11.033>.
 53. Parker, Geoffrey G. Tamm review: Leaf area index (LAI) is both a determinant and a consequence of important processes in vegetation canopies. *Forest Ecology and Management*. 2020;477(June).
 54. Available:<https://doi.org/10.1016/j.foreco.2020.118496>.
 55. Hui, Jiang, and Liu Yao. A method to upscale the leaf area index (LAI) using gf-1 data with the assistance of MODIS Products in the Poyang Lake Watershed.” *Journal of the Indian Society of Remote Sensing*. 2018;46(4):551–60.
 56. Available:<https://doi.org/10.1007/s12524-017-0731-5>.
 57. Yu, Yuanhe, Jinliang Wang, Guangjie Liu, and Feng Cheng. Forest leaf area index

- inversion based on landsat OLI data in the Shangri-La City. Journal of the Indian Society of Remote Sensing. 2019;47(6):967–76.
58. Available:<https://doi.org/10.1007/s12524-019-00950-6>.
59. Kang, Yanghui, and Mutlu Özdoğan. Field-level crop yield mapping with landsat using a hierarchical data assimilation approach. Remote Sensing of Environment. 2019;228:144–63.
60. Available:<https://doi.org/10.1016/j.rse.2019.04.005>.
61. Klingler A, Schaumberger A, Vuolo F, Kalmár LB, Pötsch EM. Comparison of Direct and Indirect Determination of Leaf Area Index in Permanent Grassland. PFG - Journal of Photogrammetry, Remote Sensing and Geoinformation Science. 2020;88(5):369–378.
62. Available:<https://doi.org/10.1007/s41064-020-00119-8>
63. Jonckheere I, Fleck S, Nackaerts K, Muys B, Coppin P, Weiss M, Baret F. Review of methods for in situ leaf area index determination Part I. Theories, sensors and hemispherical photography. Agricultural and Forest Meteorology. 2004;121(1–2):19–35.
64. Available:<https://doi.org/10.1016/J.AGRFO.2003.08.027>

© 2023 Manzi et al.; This is an Open Access article distributed under the terms of the Creative Commons Attribution License (<http://creativecommons.org/licenses/by/4.0>), which permits unrestricted use, distribution, and reproduction in any medium, provided the original work is properly cited.

Peer-review history:

The peer review history for this paper can be accessed here:
<https://www.sdiarticle5.com/review-history/108087>